

Free energy profiles of adsorption of surfactant micelles at metal-water interfaces

Himanshu Singh & Sumit Sharma

To cite this article: Himanshu Singh & Sumit Sharma (2020): Free energy profiles of adsorption of surfactant micelles at metal-water interfaces, Molecular Simulation, DOI: [10.1080/08927022.2020.1780231](https://doi.org/10.1080/08927022.2020.1780231)

To link to this article: <https://doi.org/10.1080/08927022.2020.1780231>

 View supplementary material [↗](#)

 Published online: 21 Jun 2020.

 Submit your article to this journal [↗](#)

 Article views: 15

 View related articles [↗](#)

 View Crossmark data [↗](#)



Free energy profiles of adsorption of surfactant micelles at metal-water interfaces

Himanshu Singh  and Sumit Sharma 

Department of Chemical and Biomolecular Engineering, Ohio University, Athens, OH, USA

ABSTRACT

We have studied adsorption behaviour of cationic and uncharged surfactant molecules and their micelles at metal-water interfaces via all-atom molecular dynamics (MD) simulations. Our simulations reveal that unaggregated surfactant molecules adsorb strongly on to the metal surface without any free energy barrier. The adsorption behaviour of micelles is quite different. Micelles of cationic surfactants experience a long-range free energy barrier to adsorption, which is attributed to the presence of a corona of counterions and hydration water around these micelles, which gets disturbed as the micelles approach the surface. Micelles of uncharged surfactants do not have a corona of counterions around them and therefore show a barrierless free energy profile of adsorption. The micelles of both cationic and uncharged surfactants strongly adsorb by disintegrating at the metal surface. In the disintegrated state, the molecules comprising the micelles re-arrange to attain either a lying down configuration in which the molecular axis is parallel to the surface or a standing up configuration in which the molecular axis is perpendicular to the surface.

ARTICLE HISTORY

Received 23 March 2020
Accepted 4 June 2020

KEYWORDS

Surfactant micelles; free energy of adsorption; metal-water interfaces

1. Introduction

Adsorption of surfactants on metal surfaces is useful for many technological applications, such as corrosion inhibition [1], improving selectivity in heterogeneous catalysis [2], modulating electrochemical reactions [3] and synthesis of anisotropic metal nanoparticles [4]. It is understood that surfactant molecules adsorb on polar interfaces in different morphologies, like spherical [5], cylindrical [6,7], and planar morphologies [8–11], thereby altering the interfacial thermodynamic and transport properties [12]. Relationships between molecular properties of surfactant molecules to their favoured morphologies have been analysed via theoretical considerations [13–15]. An important aspect of the problem is to understand the kinetics of adsorption of surfactants on surfaces. Experimentally, kinetics of adsorption is difficult to study using techniques like Quartz Crystal Microbalance (QCM) because the change in the mass associated with adsorbed surfactants is close to the detection limit of QCM, and, there are challenges associated with estimating the adsorbed mass accurately due to presence of hydration water around the polar groups [16,17]. Spatially-averaged conformations of molecules at interfaces can be studied via Sum Frequency Generation microscopy but these measurements are challenging to perform at metal-water interfaces and in dynamically evolving conditions [18]. The study of kinetics of adsorption of surfactants is complicated by the fact that surfactants aggregate in micelles above the critical micelle concentration (CMC). It is not understood whether the micelles adsorb directly on surfaces or undergo a morphological transformation. Formation of micelles in the bulk aqueous phase is governed by the hydrophobic effect, which may be different near interfaces [19]. In addition, favourable adsorption free energy of individual surfactant molecules

will compete with the hydrophobic interactions responsible for the integrity of the micelles. Experiments have reported a change in the adsorption behaviour near the CMC of surfactants, but the underlying reason for it is not known [20]. Previous works have shown that ionic and non-ionic surfactant molecules exhibit different adsorption behaviour on polar solid-water interfaces [21,22]. One difference in the adsorption behaviour is attributed to the adsorption of counterions on charged surfaces, which promotes stronger adsorption of ionic surfactants as compared to non-ionic surfactants [23,24].

In this work, we compare the adsorption behaviour of cationic and uncharged surfactant molecules and their micelles on metal-water interfaces by calculating their adsorption free energy profiles using molecular simulations. We have chosen imidazolium-based and quaternary ammonium-based molecules (henceforth denoted as imid and quat molecules respectively) as the cationic surfactants. These molecules are widely employed as corrosion inhibitors in oil and gas pipelines [25,26]. The structures of these molecules, along with those of uncharged amine-based surfactants (denoted as amine and triamine molecules) studied by us, are shown in Figure 1. We have performed MD simulations of these surfactants in an explicit aqueous medium and have calculated their adsorption free energy profiles on metal-water interfaces. In addition, we have studied adsorption behaviour of the micelles treated as rigid bodies to identify how the adsorption propensity changes in the absence of morphological transitions. To present a complete picture of the relevant systems, we have reviewed some of our previously published work on the adsorption behaviour of cationic surfactants [27,28] and then have compared them with the new simulation results of uncharged surfactants.

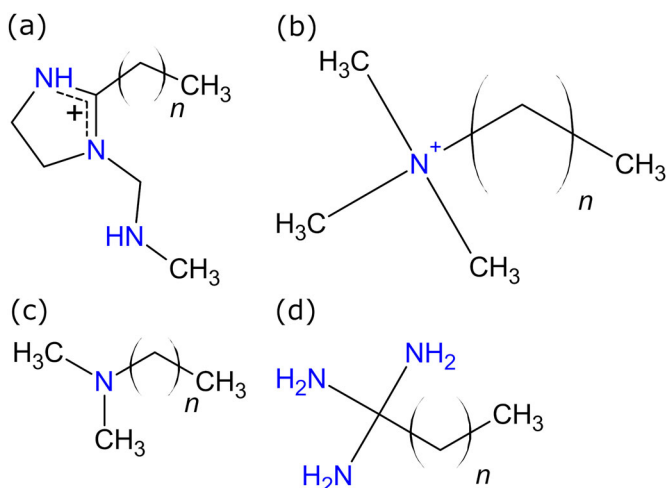


Figure 1. (Colour online) Structure of (a) imidazolium-based (imid), (b) quaternary ammonium-based (quat), (c) amine-based (amine), and (d) amine-based (tri-amine) surfactant molecules employed in this study. The subscript n indicates the length of the alkyl tail. The molecules studied by us are imid-10, imid-17, quat-10, quat-16, amine-10, triamine-10 which have 10, 17, 10, 16, 10 and 10 carbon atoms in their alkyl tails, respectively.

2. Simulation system and methods

Our simulation system comprises of surfactant molecules, water, counterions and a gold metal surface. Partial charges on the surfactant molecules are calculated from Density Functional Theory (DFT) using B3LYP hybrid functional with 6-31G(d,p) basis set and water as the implicit solvent using Gaussian 09 [29]. Interactions of the surfactant molecules are modelled using the general amber force field (GAFF) [30], a popular force field for organic molecules. Previous studies have compared thermodynamics and transport properties of different surfactant molecules obtained using molecular simulations using GAFF against experimental data, and have shown them to be in good agreement [31,32]. The metal surface is represented by six layers of gold atoms arranged in the face-centred cubic structure in the (111) plane with the lattice constant of 4.08 Å. Interactions of gold atoms are modelled using the interface force field developed by Heinz and co-workers [33], which is compatible with GAFF. Chlorides are taken as the counterions and their interactions are modelled using the Joung-Cheatham model [34]. Water molecules are represented by the Simple Point Charge Enhanced (SPC/E) model [35]. The metal surface is located at $z = 0$ plane of the simulation box and the opposite face has an athermal surface to keep the system volume constant. The simulation box is periodic in the x and y directions. The simulation box size is $66 \text{ Å} \times 65 \text{ Å} \times 150 \text{ Å}$. Total number of water molecules in the system is 15,575. We perform canonical ensemble simulations while maintaining the temperature of the system at 300 K using Nose'-Hoover thermostat. We keep a vapour space of $\sim 15 \text{ Å}$ right below the athermal surface to ensure that the system remains at saturation pressure, and thus the overall system is in the isothermal-isobaric ensemble [36]. In addition to studying surfactants near the metal surface, we have also studied their aggregation behaviour in bulk aqueous phase in the absence of a metal surface. For this system, our

simulation box is cubic in dimensions of $65 \text{ Å} \times 65 \text{ Å} \times 65 \text{ Å}$, with periodic boundary conditions in all the three directions. This system has surfactant molecules and their counter-ions in a bath of 9200 water molecules. In case of uncharged surfactant molecules, no counterions are included in the simulation system. A spherical cutoff of 10 Å is chosen for Lennard Jones (LJ) and real space part of Coulombic interactions. The k -space part of Coulombic interactions is computed using the particle-particle particle-mesh (PPPM) method. All MD simulations are performed using the large-scale atomic/molecular massively parallel simulator (LAMMPS) software package [37].

3. Results and discussion

In straightforward MD simulations of N quaternary ammonium (quat) and imidazolium (imid) type surfactant molecules near a metal surface ($N = 60$), it is observed that a few surfactant molecules adsorb on the metal surface while the remaining molecules aggregate in the aqueous phase as almost spherical micelles [27,28]. These micelles do not adsorb on the surface during the course of the simulations, which suggests that the adsorption behaviour of unaggregated surfactant molecules is different from their micelles. Therefore, we have studied the adsorption behaviour of unaggregated molecules and their micelles by performing independent free energy calculations.

3.1. Adsorption free energy profiles in infinite dilution

We have calculated adsorption free energy profiles of surfactant molecules in infinite dilution using umbrella sampling [27]. In this calculation, we restrain a surfactant molecule at a distance ξ from the surface using a harmonic potential. The biasing potential on a configuration i restrained at ξ is given by,

$$V_{bias} = k(\xi_i - \xi)^2 \quad (1)$$

where ξ_i is the location of the centre of mass of the molecule in the configuration i . To sample the umbrella sampling windows, the ξ is varied from 3 Å to 25 Å in a series of simulations. For $\xi > 15 \text{ Å}$, the simulations are performed using the harmonic force constant, $k = 5 \text{ kcal/mol/Å}^2$ and with ξ varying in increments of 1 Å . For $\xi \leq 15 \text{ Å}$, the simulations are performed with the force constants, $k = 10, 25$ and 50 kcal/mol/Å^2 and with ξ varying in increments of 0.5 Å . Larger values of k are needed for $\xi \leq 15 \text{ Å}$ because the molecules show a strong tendency to adsorb and thus more restraining force is needed to adequately sample these locations. For each value of ξ , an equilibrium run of 20 ns is performed, which is followed by a production run of 40 ns. The free energy profiles are generated using the Weighted Histogram Analysis Method (WHAM) [27]. Figure 2 shows the resultant adsorption free energy profiles of quat-10 and quat-16 molecules in infinite dilution on the metal surface [38]. It is observed that the surfactant molecules adsorb strongly ($\Delta G \approx -35 k_B T$) without experiencing any free energy barrier. Similar adsorption free energy profiles have been reported by us for the imid molecules [27]. The inset image shows a snapshot of a quat-10 molecule in the adsorbed

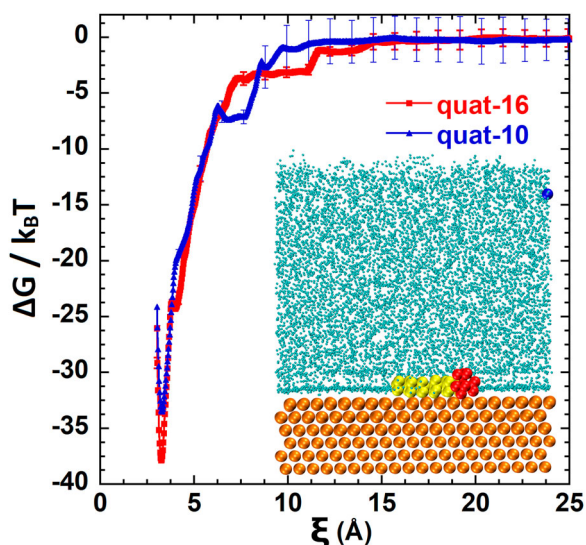


Figure 2. (Colour online) Adsorption free energy profiles of quat-10 and quat-16 molecules in infinite dilution on a gold lattice; inset: equilibrium adsorbed configuration of the quat-10 molecule. Error bars are calculated by generating three independent free energy profiles. The centres of metal atoms in the topmost layer of the metal surface are located at $\xi = 0$ Å. Water molecules are represented in cyan colour and the gold lattice is represented by orange beads. The blue bead represents the counterion, chloride.

state. It is seen that the most favourable configuration of the molecule is to lie flat on the surface.

3.2. Adsorption free energy profiles of surfactant micelles

As discussed above, our straightforward MD simulations have revealed that the surfactant molecules aggregate in micelles in the aqueous phase. To study their aggregation tendency, we have performed simulations of these molecules in the bulk aqueous phase in the absence of a metal surface. Our MD simulations of imid and quat type surfactants show that these molecules aggregate in micelles of 18–19 molecules. We do not get larger micelles even when a simulated annealing is performed from 400 K to 300 K in steps of 10 K [27,28]. From the radius of gyration tensor of these micelles, the asphericity values are found to be close to 0.15, indicating that these micelles are nearly spherical and have a radius of ~ 15 Å [27,28]. The uncharged molecules also form spherical micelles. The asphericity values of amine-10 and triamine-10 micelles, each comprising of 18 molecules are 0.13 and 0.15 respectively. Unlike the cationic surfactants, the uncharged molecules are able to form micelles of size larger than 18 molecules. The inability of cationic surfactants to form larger micelles is probably due to the unfavourable Coulombic interactions between the surfactant molecules [39]. The micelles of uncharged surfactants have a higher packing density. The number densities (number of heavy atoms per unit volume of micelle) of amine-10 and triamine-10 micelles comprising of 18 molecules are 0.37 heavy atoms/Å³ and 0.33 heavy atoms/Å³ respectively, whereas those of imid-10 and quat-10 micelles are 0.28 heavy atoms/Å³ and 0.26 heavy atoms/Å³ respectively [39]. Figure 3 shows snapshots of the different surfactant micelles formed in our simulations. The polar head groups can be seen pointing

outwards towards the aqueous phase. This result is supported in Figure S1 (Supporting Information), which shows the distribution of polar head groups as a function of their distance from the centre of mass of the micelles.

3.2.1. Micelles of cationic surfactants

To calculate the free energy profiles of adsorption of micelles, we place one micelle in the aqueous phase at different distances from the metal surface, ξ . The micelle is restrained close to ξ via the above described umbrella sampling methodology but with the modification that now the biasing potential (equation (1)) is applied to the centre of mass of the micelle. In these simulations, for $\xi > 25$ Å, the harmonic force constant, $k = 5$ kcal/mol/Å² is used and ξ is varied in increments of 1 Å. For $\xi \leq 25$ Å, we have employed $k = 10, 25,$ and 50 kcal/mol/Å² and with ξ varied in increments of 0.5 Å. At each location, an equilibrium run of 40 ns is followed by a production run of 40 ns, except at distances close to the surface ($\xi \leq 20$ Å), wherein a longer equilibrium run (~ 100 – 200 ns) is needed to attain equilibrium configuration of the micelles. Figure 4 shows the adsorption free energy profiles of the imid-17 and quat-10 micelles [28].

It is observed in Figure 4 that the cationic micelles experience a repulsion from the metal surface even up to $\xi = 50$ Å. Since the radius of the micelles is ~ 15 Å, this is a long-range repulsion. This long-range repulsion is attributed to the presence of a solvation shell of counter-ions and water molecules surrounding the micelle, which interacts with the adsorbed layers of water on the metal surface [27,28] (kindly refer Figures S2–S4 (Supporting Information) that show the radial distribution functions of counterions around the polar head, water molecules around the counterions and the adsorbed layers of water on the metal surface). Once this barrier is overcome, Figure 4 shows that the free energy of adsorption of the micelles is favourable. It is observed that the micelles adsorb strongly by disintegrating at the metal surface. The complete disintegration of the micelles occurs in a timescale of ~ 200 ns [28]. Figure 5 shows snapshots of the imid-17 micelle obtained from an unbiased simulation at different times when the micelle is initially placed on the metal surface. The snapshots show that the imid-17 micelle completely disintegrates on the metal surface over time. Upon disintegration, the constituent molecules of the micelle lie flat on the metal surface. A movie of the disintegration of the micelle is shown in Movie S1.

It is to be noted that the free energy profiles in Figure 4 are plotted only up to $10 k_B T$ in order to show the long-range free energy barrier clearly. The true minimum of the free energy profiles would be a much lower value, approximated to be the summation of the adsorption free energies of all the constituent molecules. Disintegration of micelles at metal-water interfaces can be understood by comparing the free energy associated with the formation of a micelle in the bulk phase ($\Delta G_{\text{micellization}}$) with the free energy of the molecules adsorbing on the surface ($\Delta G_{\text{adsorption}}$). We have previously calculated $\Delta G_{\text{micellization}}$ of an imid-10 micelle comprising of $N = 18$ molecules to be $\sim -68 k_B T$ [38]. $\Delta G_{\text{adsorption}}$ for these molecules will be $N \times (-30) k_B T \sim -540 k_B T$ [27]. Hence, $\Delta G_{\text{adsorption}} \ll \Delta G_{\text{micellization}}$, which suggests that the micelle has a tendency to disintegrate upon adsorption on the metal surface.

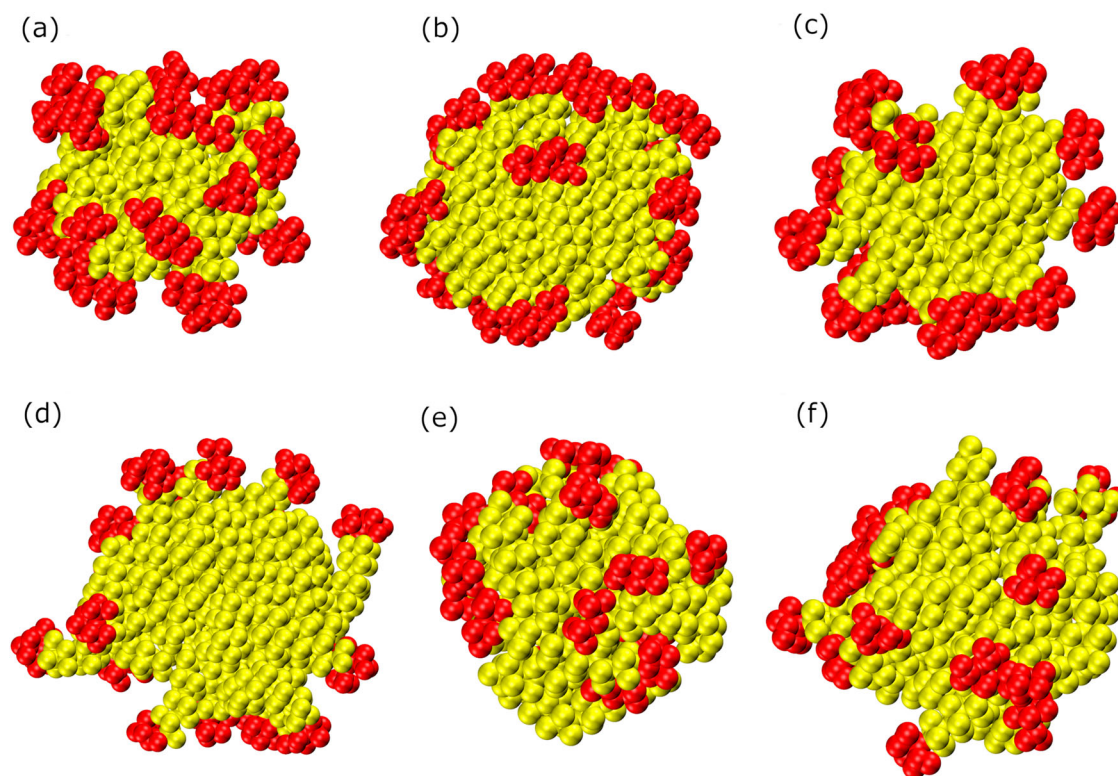


Figure 3. (Colour online) Snapshots of (a) an imid-10 micelle, (b) an imid-17 micelle, (c) a quat-10 micelle, (d) a quat-16 micelle, (e) an amine-10 micelle, and (f) a triamine-10 micelle, respectively. Red beads represent the polar head groups, and the yellow beads represent the alkyl tails.

Experiments have reported that quaternary ammonium surfactants adsorb on a gold surface in the lying-down configuration, similar to our simulation results [40].

To prove that the disintegration of the micelles is responsible for their strong adsorption, we calculate the adsorption free energy profiles of the micelles by treating them as rigid bodies. We create a rigid micelle by selecting a configuration of the non-rigid micelle which has the same values of asphericity and squared radius of gyration as the averaged values of the non-rigid micelle in the bulk aqueous phase. In a rigid micelle, all intra-molecular interactions are set to zero. The external

forces and torques act on the centre of mass of the micelle. Hence, a rigid micelle cannot deform like the non-rigid micelle. Free energy profiles of adsorption of the rigid and the non-rigid imid-10 and quat-16 micelles are shown in Figure 6 [28].

It is observed in Figure 6 that there is a long-range free energy barrier to adsorption of the rigid micelles, as in the case of the non-rigid micelles. However, the adsorption free energy of the rigid micelles is much smaller in comparison to the non-rigid micelles. This confirms our assertion that when the micelles do not disintegrate, they only have a weak tendency to adsorb on the metal surface. Another difference that is

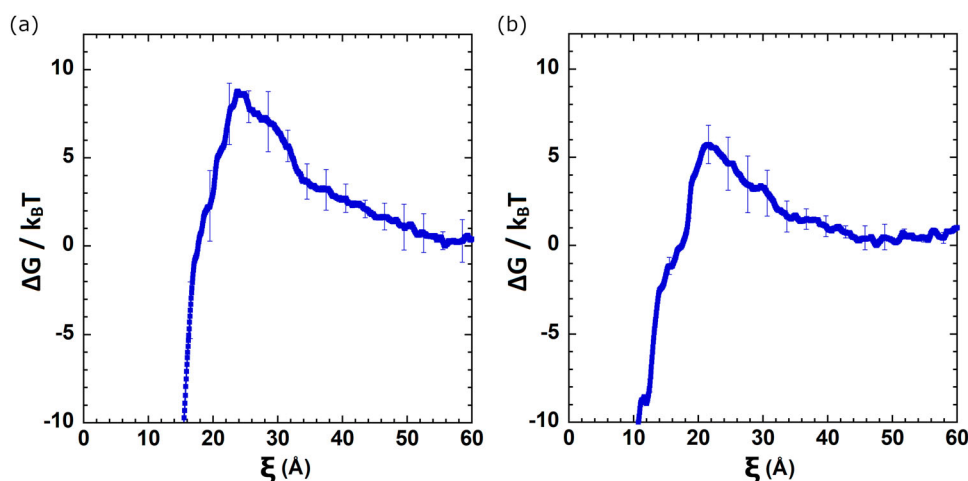


Figure 4. (Colour online) Free energy profiles of the adsorption of (a) imid-17, and (b) quat-10 micelles. Error bars are calculated by generating three independent free energy profiles. Adapted with permission from Singh and Sharma [28]. Copyright (2020) American Chemical Society.

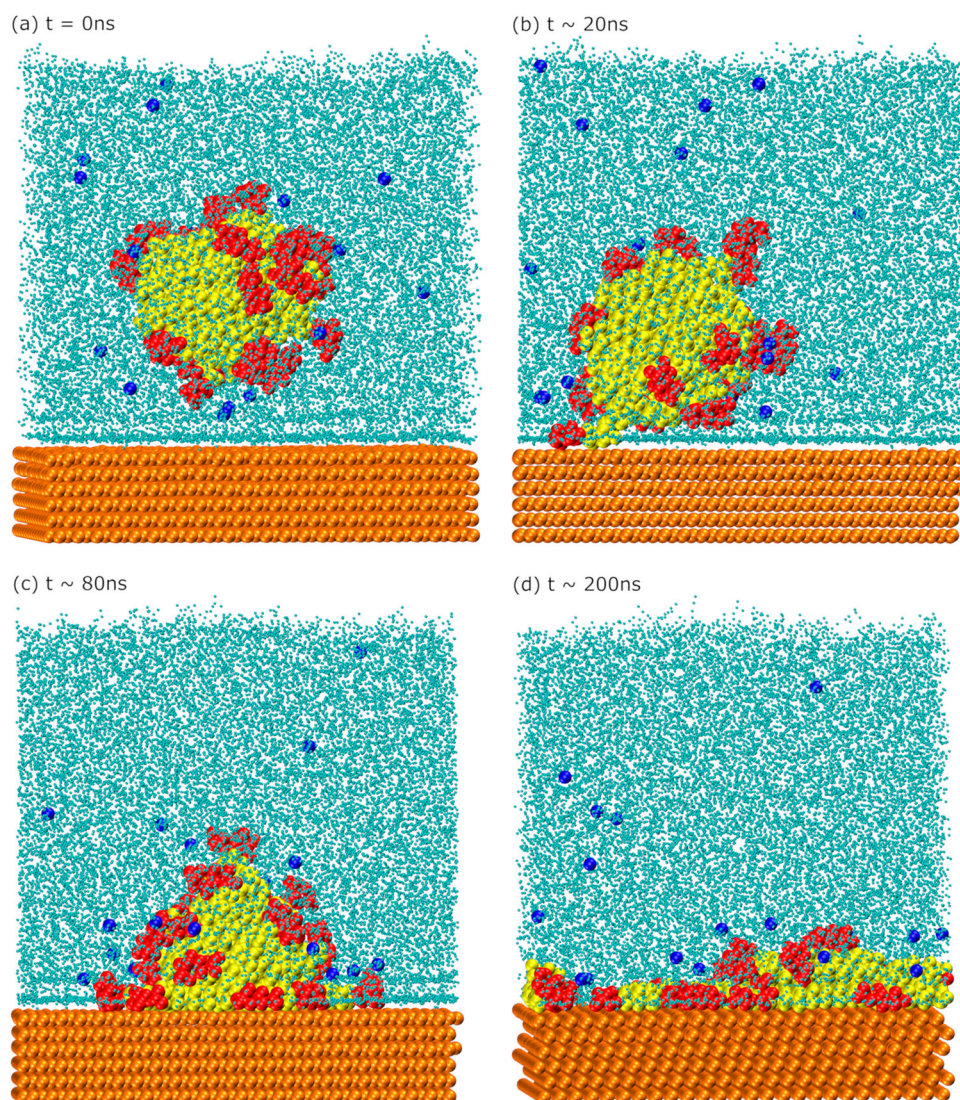


Figure 5. (Colour online) Unbiased MD simulation showing the adsorption and disintegration of imid-17 micelle on the metal surface. Adapted with permission from Singh and Sharma [28]. Copyright (2020) American chemical Society.

noticed is that the free energy barrier of the rigid micelles is larger and has a peak at 18 \AA as opposed to 22 \AA in the case of the non-rigid micelles. At this peak, the micelles partially lose their solvation shell because of their proximity to the metal surface. In the case of non-rigid micelles however, this loss in energetics is compensated by the rearrangement of the molecules comprising the micelle. The absence of this rearrangement in the case of rigid micelles results in a larger free energy barrier.

Free energy profiles for the rigid micelles are only ascertained up to 15.5 \AA from the metal surface because that is the closest distance that these micelles can attain owing to their rigidity. Figure 7 shows the equilibrium adsorbed morphology of a (a) rigid micelle and (b) a non-rigid micelle on the metal surface. The non-rigid imid-17 micelle is disintegrated with its molecules lying flat on the surface.

3.2.2. Micelles of uncharged surfactants

In the previous section, we show that the cationic micelles experience a long-range free energy barrier to adsorption because of the presence of a large corona of counter-ions and

water molecules in their solvation shell. In this section, we discuss the adsorption free energy profiles of micelles of uncharged molecules that do not have a corona of counterions. We have studied the adsorption behaviour of amine-10 and triamine-10 micelles (Figure 3). Each micelle studied by us comprises of 18 molecules. Figure 8(a) shows the adsorption free energy profiles of the non-rigid and the rigid amine-10 micelles, and Figure 8(b) shows the adsorption free energy profile of the non-rigid triamine-10 micelle.

Interestingly, it is observed that there is no free energy barrier to the adsorption of the uncharged micelles, which suggests that the free energy barrier in the case of cationic micelles is due to the corona of the counterions. Figure 8(a) also shows that the rigid amine-10 micelle has a weaker adsorption free energy as compared to the non-rigid micelle, highlighting that the disintegration of the micelles is responsible for their strong adsorption. The free energy profiles for the non-rigid micelles is plotted only up to $14 k_B T$ in order to clearly highlight the difference between the profiles of the rigid and the non-rigid micelles. These free energy profiles

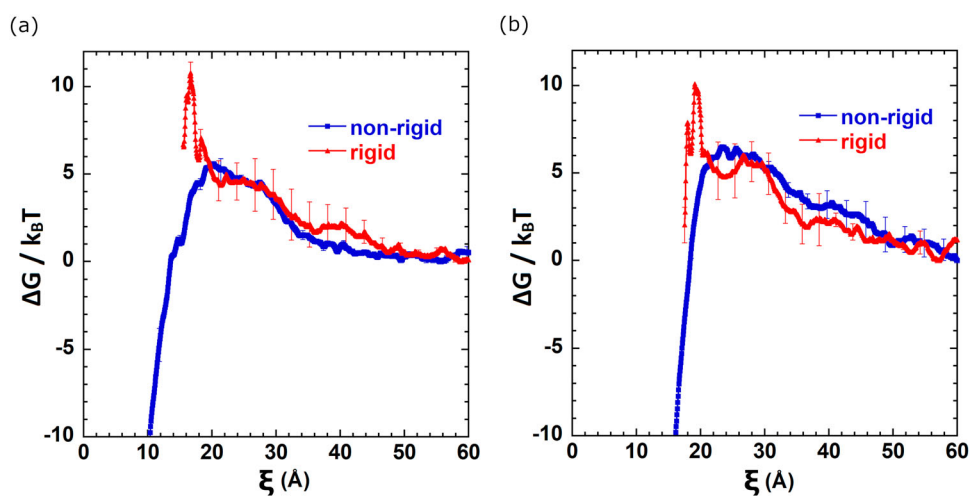


Figure 6. (Colour online) Free energy profiles of adsorption of the rigid and the non-rigid micelles of (a) imid-10, and (b) quat-16 molecules. The error bars are determined from three independent free energy profiles. Adapted with permission from Singh and Sharma [28]. Copyright (2020) American Chemical Society.

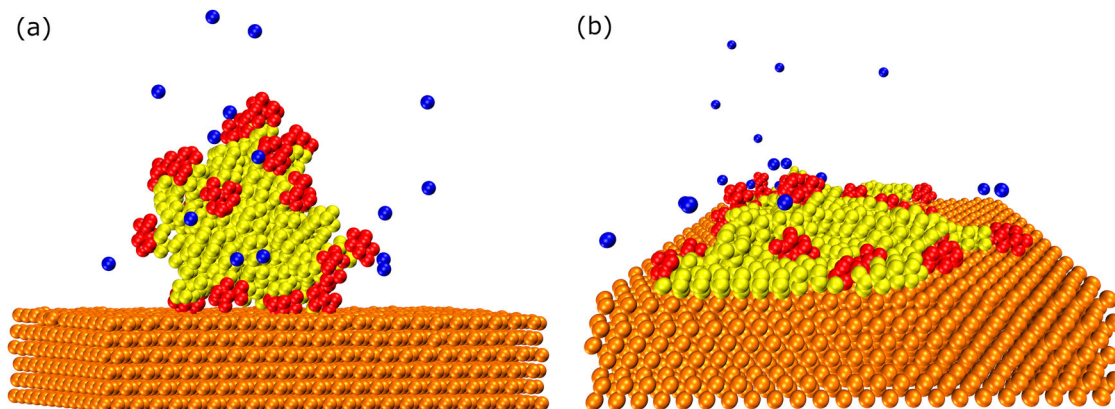


Figure 7. (Colour online) Snapshot of (a) a rigid quat-16 micelle, and (b) a non-rigid imid-17 micelle adsorbed on the metal surface at equilibrium. Water molecules are not shown for clarity. Adapted with permission from Singh and Sharma [28]. Copyright (2020) American Chemical Society.

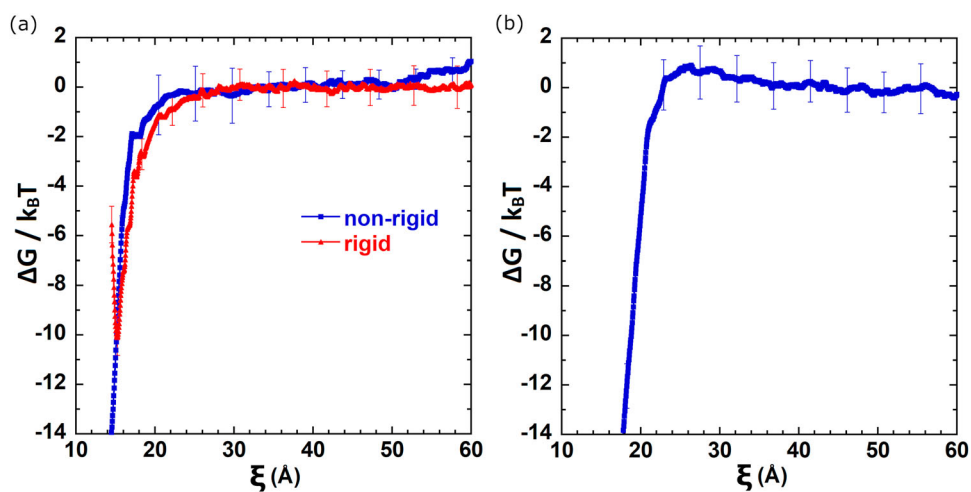


Figure 8. (Colour online) Free energy profiles of the adsorption of (a) the rigid and the non-rigid amine-10 micelles, and (b) the non-rigid triamine-10 micelle. The error bars are determined from three independent free energy profiles.

suggest that the adsorption of uncharged micelles is kinetically favoured over the adsorption of cationic surfactants on uncharged metal surfaces.

Figure 9 depicts the equilibrium morphology of the uncharged micelles in the adsorbed state after an unbiased simulation run of 200 ns. The amine micelle is disintegrated

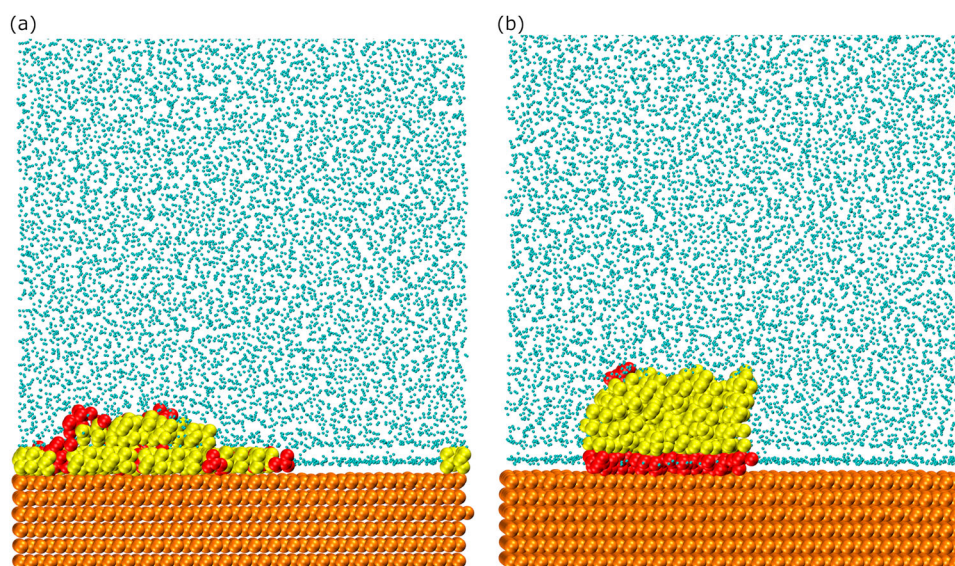


Figure 9. (Colour online) Snapshot of (a) an amine-10 micelle, and (b) a triamine-10 micelle disintegrated on the metal surface. Amine-10 molecules lie flat, while the triamine-10 molecules stand up on the surface.

with its molecules lying flat on the surface. On the other hand, the triamine micelle is disintegrated with its molecules standing up on the surface, with most of the polar head groups (17 out of 18) pointing down towards the metal and the hydrophobic tails pointing up towards the bulk aqueous phase. Figure S5 (Supporting Information) shows the average orientation of the molecules in the adsorbed state of the micelles. Movie S2 shows the kinetics of disintegration of the triamine micelle on the metal surface, where the micelle rearranges in a way that its constituent molecules stand up on the surface.

The difference between an amine and a triamine molecule is their polar head group. The triamine molecule has three amine groups which makes it a strongly polar group as compared to the amine molecule, which has only one amine group. The orientation of the molecules on the surface depends upon the strength of interaction of their polar head groups with the metal surface [14]. The triamine molecules prefer to stand-up on the surface because in the lying-down configuration, the interaction of the head group with the surface is weaker as only one nitrogen can be in contact with the surface. The kinetics of adsorption of the triamine micelle suggests how the islands of molecules standing-up on the surface, as reported in the experiments may form during the adsorption process.

4. Conclusions

We have studied adsorption behaviour of surfactants at metal-water interfaces using atomistic simulations. We report that the adsorption behaviour depends on the aggregated state of the surfactants. In the unaggregated state, the molecules have a strong tendency to adsorb without any free energy barrier. Micelles of cationic surfactants experience a long-range free energy barrier to adsorption on an uncharged metal surface because they have a corona of counterions surrounding the micelles which gets disturbed as the micelles approach the surface. Uncharged micelles, devoid of a corona of counterions show a barrierless adsorption free energy profile. In addition,

we show that the micelles adsorb strongly on to the metal surface upon disintegration. Rigid micelles, which cannot disintegrate, show only a weak tendency towards adsorption. Finally, we show that in the disintegrated state, the surfactant molecules can attain a lying-down configuration or a standing-up configuration depending upon the strength of interaction of their head groups with the metal surface.

Acknowledgements

This work is supported by the NSF CBET grant 1705817. The authors thank researchers at the Institute for Corrosion and Multiphase Technology (ICMT) for useful discussions. Computational resources for this work were provided by the Ohio Supercomputer Center and National Science Foundation XSEDE grant number DMR190005.

Disclosure statement

No potential conflict of interest was reported by the author(s).

Funding

This work was supported by Division of Chemical, Bioengineering, Environmental, and Transport Systems [grant number 1705817]; Division of Materials Research [grant number DMR190005].

ORCID

Himanshu Singh  <http://orcid.org/0000-0002-8437-686X>
Sumit Sharma  <http://orcid.org/0000-0003-3138-5487>

REFERENCES

- [1] Malik MA, Hashim M, Nabi F, et al. Anti-corrosion ability of surfactants: a review. *Int J Electrochem Sci.* 2011;6(6):1927–1948.
- [2] Thomas JM, Thomas WJ. Principles and practice of heterogeneous catalysis. New York (NY): John Wiley & Sons; 2014.
- [3] Franklin TC, Mathew S. The use of surfactants in electrochemistry, in surfactants in solution. New York (NY): Springer; 1989; p. 267–286.

- [4] Johnson CJ, Dujardin E, Davis SA, et al. Growth and form of gold nanorods prepared by seed-mediated, surfactant-directed synthesis. *J Mater Chem*. 2002;12(6):1765–1770.
- [5] Manne S, Gaub HE. Molecular organization of surfactants at solid-liquid interfaces. *Science*. 1995;270(5241):1480–1482.
- [6] Manne S, Cleveland JP, Gaub HE, et al. Direct visualization of surfactant hemimicelles by force microscopy of the electrical double layer. *Langmuir*. 1994;10(12):4409–4413.
- [7] Jaschke M, Butt H-J, Gaub HE, et al. Surfactant aggregates at a metal surface. *Langmuir*. 1997;13(6):1381–1384.
- [8] Xiong Y, Brown B, Kinsella B, et al. Atomic force microscopy study of the adsorption of surfactant corrosion inhibitor films. *Corrosion*. 2014;70(3):247–260.
- [9] Hayes WA, Schwartz DK. Two-stage growth of octadecyltrimethylammonium bromide monolayers at mica from aqueous solution below the krafft point. *Langmuir*. 1998;14(20):5913–5917.
- [10] Xu S, Cruchon-Dupeyrat SJN, Garno JC, et al. In situ studies of thiol self-assembly on gold from solution using atomic force microscopy. *J Chem Phys*. 1998;108(12):5002–5012.
- [11] Xu S-L, Wang C, Zeng Q-D, et al. Self-assembly of cationic surfactants on a graphite surface studied by STM. *Langmuir*. 2002;18(3):657–660.
- [12] Murphy CJ, Sau TK, Gole AM, et al. Anisotropic metal nanoparticles: synthesis, assembly, and optical applications. *J Phys Chem B*. 2005;109(29):13857–13870.
- [13] Johnson RA, Nagarajan R. Modeling Self-assembly of surfactants at solid-liquid interfaces. II. hydrophilic surfaces. *Colloid Surface A*. 2000;167(1–2):21–30.
- [14] Sharma S, Singh H, Ko X. A quantitatively accurate theory to predict adsorbed configurations of linear surfactants on polar surfaces. *J Phys Chem B*. 2019;123(34):7464–7470.
- [15] Ko X, Sharma S. Adsorption and self-assembly of surfactants on metal-water interfaces. *J Phys Chem B*. 2017;121(45):10364–10370.
- [16] Caruso F, Serizawa T, Furlong DN, et al. Quartz crystal microbalance and surface plasmon resonance study of surfactant adsorption onto gold and chromium oxide surfaces. *Langmuir*. 1995;11(5):1546–1552.
- [17] Stålgren JJR, Eriksson JC, Boschkova K. A comparative study of surfactant adsorption on model surfaces using the quartz crystal microbalance and the ellipsometer. *J Colloid Interf Sci*. 2002;253(1):190–195.
- [18] Khan MR, Premadasa UI, Cimatu KLA. Role of the cationic head-group to conformational changes undergone by shorter alkyl chain surfactant and water molecules at the air-liquid interface. *J Colloid Interf Sci*. 2020;568:221–233.
- [19] Vembanur S, Patel AJ, Sarupria S, et al. On the thermodynamics and kinetics of hydrophobic interactions at interfaces. *J Phys Chem B*. 2013;117(35):10261–10270.
- [20] Knag M, Sjöblom J, Øye G, et al. A quartz crystal microbalance study of the adsorption of quaternary ammonium derivatives on iron and cementite. *Colloid Surface A*. 2004;250(1–3):269–278.
- [21] Huang L, Maltesh C, Somasundaran P. Adsorption behavior of cationic and nonionic surfactant mixtures at the alumina-water interface. *J Colloid Interf Sci*. 1996;177(1):222–228.
- [22] Somasundaran P, Snell ED, Fu E, et al. Effect of adsorption of non-ionic surfactant and non-ionic—anionic surfactant mixtures on silica—liquid interfacial properties. *Colloid Surface*. 1992;63(1–2):49–54.
- [23] Paria S, Khilar KC. A review on experimental studies of surfactant adsorption at the hydrophilic solid-water interface. *Adv Colloid Interfac*. 2004;110(3):75–95.
- [24] Singh A, Ansari KR, Xu X, et al. An impending inhibitor useful for the oil and gas production industry: weight loss, electrochemical, surface and quantum chemical calculation. *Sci Rep-UK*. 2017;7(1):1–17.
- [25] Cruz J, Martí'nez R, Genesca J, et al. Experimental and theoretical study of 1-(2-ethylamino)-2-methylimidazoline as an inhibitor of carbon steel corrosion in acid media. *J Electroanal Chem*. 2004;566(1):111–121.
- [26] Hegazy MA, Abdallah M, Awad MK, et al. Three novel di-quaternary ammonium salts as corrosion inhibitors for API X65 steel pipeline in acidic solution. Part I: experimental results. *Corros Sci*. 2014;81:54–64.
- [27] Kurapati Y, Sharma S. Adsorption free energies of imidazolium-type surfactants in infinite dilution and in micellar state on gold surface. *J Phys Chem B*. 2018;122(22):5933–5939.
- [28] Singh H, Sharma S. Disintegration of surfactant micelles at metal-water interfaces promotes their strong adsorption. *J Phys Chem B*. 2020;124:2262–2267.
- [29] Frisch MJ, Trucks GW, Schlegel HB, et al. Gaussian~ 09 revision D. 01. 2014.
- [30] Wang J, Wolf RM, Caldwell JW, et al. Development and testing of a general amber force field. *J Comput Chem*. 2004;25(9):1157–1174.
- [31] Sprenger KG, Jaeger VW, Pfandner J. The general AMBER force field (GAFF) can accurately predict thermodynamic and transport properties of many ionic liquids. *J Phys Chem B*. 2015;119(18):5882–5895.
- [32] Babiacyk WI, Bonella S, Guidoni L, et al. Hydration structure of the quaternary ammonium cations. *J Phys Chem B*. 2010;114(46):15018–15028.
- [33] Heinz H, Vaia RA, Farmer BL, et al. Accurate simulation of surfaces and interfaces of face-centered cubic metals using 12– 6 and 9– 6 Lennard-Jones potentials. *J Phys Chem C*. 2008;112(44):17281–17290.
- [34] Joung IS, Cheatham III TE. Determination of alkali and halide monovalent ion parameters for use in explicitly solvated biomolecular simulations. *J Phys Chem B*. 2008;112(30):9020–9041.
- [35] Berendsen HJC, Grigera JR, Straatsma TP. The missing term in effective pair potentials. *J Phys Chem*. 1987;91(24):6269–6271.
- [36] Patel AJ, Varilly P, Chandler D. Fluctuations of water near extended hydrophobic and hydrophilic surfaces. *J Phys Chem B*. 2010;114(4):1632–1637.
- [37] Plimpton S. Fast parallel algorithms for short-range molecular dynamics. Albuquerque (NM, USA): Sandia National Labs; 1993.
- [38] Singh H, Kurapati Y, Sharma S. Aggregation and adsorption behavior of organic corrosion inhibitors studied using molecular simulations. NACE Corrosion Conference; 2019.
- [39] Sharma S, Ko X, Kurapati Y, et al. Adsorption behavior of organic corrosion inhibitors on metal surfaces—some new insights from molecular simulations. *Corrosion*. 2019;75(1):90–105.
- [40] Chen M, Burgess I, Lipkowski J. Potential controlled surface aggregation of surfactants at electrode surfaces—a molecular view. *Surf Sci*. 2009;603(10–12):1878–1891.